Review Article

The S_N2 and Single Electron Transfer Concepts. A Theoretical and Experimental Overview

Sason S. Shaik*

Department of Chemistry, Ben-Gurion University, Beer Sheva 84105, Israel

Shaik, S. S., 1990. The S_N2 and Single Electron Transfer Concepts. A Theoretical and Experimental Overview. – Acta Chem. Scand. 44: 205–221.

This review discusses reactivity patterns in and relationships between S_N2 and SET (single electron transfer) reactions of $Y:^-/R–X$ reactant pairs. The curve-crossing diagram is used to model the activation process as distortions and solvent reorganizational modes which are required to lead to crossing (resonance) of the ground and charge transfer states. The resonance condition can be achieved by a 'complete' distortion which involves the umbrella inversion, the C–X cleavage, the Y–C bond coupling, and the solvent reorganizational modes. This is the synchronous S_N2 or *single electron shift mechanism*. Much of S_N2 reactivity is shown to be in accord with this picture. Alternatively, the resonance condition between the ground and charge transfer states can be achieved by distortions that are devoid of bond coupling. This is the *single electron transfer* (SET) *mechanism*, in which the electron transfer step precedes the bond coupling step. The various factors which affect the competition between the two mechanisms are discussed. Appropriate structural types are discussed which possess zero degree of avoided crossing and can thereby qualify as SET transition states. Orbital-symmetry factors are considered and it is suggested that SET transition states can be obtained by trajectories which minimize the HOMO–LUMO interaction between $Y:^-$ and R–X. The role of coordination of $Y:^-$ and R–X in ion-pairing aggregates is discussed in terms of the minimization of the HOMO–LUMO interaction. Other roles of counterions (e.g., Li^+), as promoting SET transition states are also discussed. We conclude that the S_N2 and SET mechanisms, for $Y:^-/RX$ reactant pairs, are electronically related and their transition states are structurally isomeric, respectively maximizing and minimizing the HOMO ($Y:^-$)–LUMO (R–X) interaction.

The relationship between S_N2 and single electron transfer (SET) reactions is a fundamental problem in contemporary physical organic chemistry.[1] An initial suggestion by Bank and Noyd[2] in 1973 that there exists such a relationship for *typical* S_N2 systems was soon rejected only to enjoy rejuvenation in recent years, albeit in modified forms, by both experimental and theoretical investigations (a list of the various contributions is necessarily going to be incomplete and is given up at this point). In fact the kinship between polar and SET mechanisms is not restricted to aliphatic nucleophilic substitution, but appears to be the tip of an emerging iceberg that is observed in the broader area of electrophilic–nucleophilic reactivity.[3–8] It is essential, as such, to understand the S_N2/SET relationship as a prototype of a major chemical trend.

To understand the factors that govern reactivity patterns in the S_N2 and SET mechanisms, and the nature of their relationship, one must first define the essence of the activation process and then demonstrate how the various structure/reactivity patterns spring from that definition. In 1981 it was shown that the activation barrier for reactions which involve nucleophile–electrophile combinations can be modelled in a unified manner as a result of the avoided crossing[9] between the *ground and charge transfer states of the reactants*. Polar and SET mechanisms have therefore a common link, in the sense that they both involve activation which is associated with the single electron 'movement.'

The curve-crossing model has been subsequently developed and applied to a variety of reactions.[10–13] The S_N2 reaction has received the most extensive treatment[10,12] that has shown that the modelling of the barrier as a result of avoided crossing of ground and charge transfer states provides a unified framework for conceptualizing the variety of observed reactivity patterns in the gas phase and in solution. The S_N2 reaction has been therefore called *'a single electron shift'* mechanism[1,10–12] which means that the single electron 'movement' occurs in a single step which also involves the bond coupling between the nucleophile and the substrate, as opposed to the SET mechanism, where the single electron 'movement' precedes the bond coupling. Recently, the curve-crossing model has been used[1,14] to project the relationship between the two mechanisms and analyze factors which prefer one mechanism over the other. The above publications coincided with intense activity and interest in the dichotomy between the two mechanisms – a dichotomy which is gradually becoming a central and sometimes controversial[15] theme in physical organic

* In part, presented as a main section lecture at the 32nd IUPAC Congress in Stockholm, Sweden, August 2–7, 1989.

chemistry (see for example chapters V and VII in Ref. 6).

This paper reviews the current status of the curve-crossing view of the S_N2/SET relationship, based on previous publications[1,10] and new material on the reactivity patterns in the two mechanistic classes.

The identity S_N2 reaction of methyl derivatives

The barrier of the identity exchange [eqn. (1)] is of fundamental significance, as it represents the net outcome of electronic reorganization, unmasked by thermodynamic effects.

$$X:^- + R\text{–}X \rightarrow X\text{–}R + :X^- \qquad (1)$$

The observed reactivity patterns[10,16–20] show a few interesting trends. The relative reactivity in a set of identity reactions [eqn. (1)] follows the 'leaving-group ability' of X but is unrelated to its 'nucleophilicity.' In accord, small barriers have been found for X = I, Br, Cl, while large ones have been evaluated for X = F, OH, CH_3O, HS, CH_3S, CN, CCH, $PhCH_2$. The reactivity trends appear to be medium independent, and persist in the gas phase,[17] in a 'vacuum',[20] and in a variety of solvents.[18,19] In the following sections we show how these trends can be reconstructed and predicted by use of the curve-crossing diagram, and in what way are they related to fundamental charge-transfer properties of the reactants and the solvent.

The activation process. Fig. 1 is the curve-crossing diagram which by avoided crossing generates the central barrier and the reaction profile for the identity S_N2 process.[10,16] Following the introductory section, the upper anchor states in the diagram are *vertical* charge-transfer states, generated by transferring a single electron from $X:^-$ to the valence σ_{CX}^* orbital of the R–X molecule. This vertical charge transfer state is shown in **1** where the dashed line indicates that the two odd electrons are paired up to a singlet (the singlet-paired spin state is the linear combination $\alpha\beta$–$\beta\alpha$, and we therefore do not specify the spins of the odd electrons in **1**. Instead, the spin pairing is indicated by the dashed line).

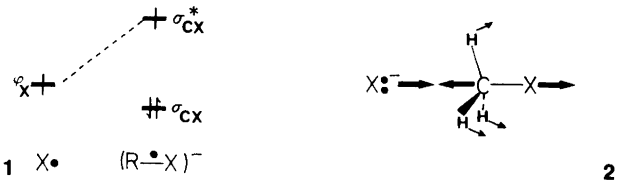

1 **2**

The simplest expression for the central barrier is eqn. (2) which states that the barrier is given by the difference between the energy of the crossing point, ΔE_c, and the avoided crossing interaction, B. In turn, the height of the crossing point simply corresponds to a fraction, f, of the vertical electron transfer energy gap, $I_{X:}^* - A_{RX}^*$ (asterisks signify a vertical property).

$$\Delta E^{\neq} = \Delta E_c - B;\ \Delta E_c = f(I_{X:}^* - A_{RX}^*) \qquad (2)$$

At the crossing point of Fig. 1, the ground and charge-transfer states are in resonance, which is a condition for generating the transition state.[9,10] It is by resonance that the electrons, which are initially localized in their reactant form, can be reorganized and give equal weight to the product form, so that finally beyond the crossing point the electrons can be paired up anew in the product form. Since the ground and charge transfer states are initially separated by the vertical electron transfer energy gap, the requisite resonance must be achieved by distortion mechanisms which stabilize the charge transfer state and destabilize the ground state, so that the gap is overcome and crossing is attained.

If we restrict our attention to the gas phase S_N2 reaction, then the distortion mechanism is simply the reaction coordinate mode shown by the thick arrows in **2**. That the ground state should be destabilized by the distortions depicted in **2** is self-evident. The charge-transfer state is stabilized by the distortion due to two effects. Firstly, the radical anion $(R\text{–}X)^-$ is itself stabilized because the bond-stretching deformation relaxes the antibonding character of the occupied σ^* orbital, in **1**, and secondly, by the approach of the reactants the two spin-paired electrons, of X· and $(R\text{–}X)^-$ in **1**, lead to stabilization as they are coupled into a covalent X–R bond at the opposite side of R.

Thus, the S_N2 distortion (**2**) provides the resonance or crossing mechanism between the ground and charge-transfer states. The height of the crossing points is then the distortion energy which is required to destabilize the ground state such that it achieves resonance with the descending charge-transfer state. In turn, the avoided cross-

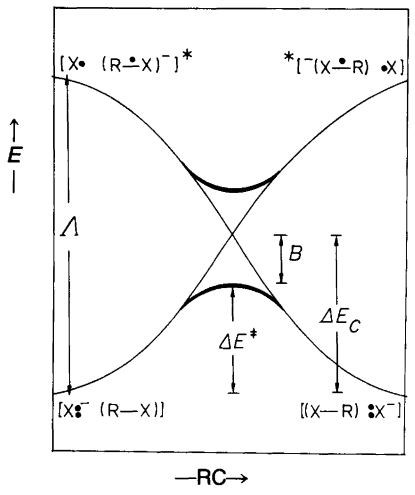

Fig. 1. A curve crossing diagram for an identity S_N2 reaction. The ground states are the ion–dipole encounter complexes, while the excited states are vertical charge transfer states. In solution, these states become $[X:^-\ (R\text{–}X)](s)$ and $[X\cdot\ (R\text{–}X)^-](s^*)$, where (s) and (s*) denote equilibrium and non-equilibrium solvation. The gap, Λ, is given by the the difference between the vertical ionization potential ($I_{X:}^*$) and electron affinity (A_{RX}^*). The thick lines correspond to the states after avoided crossing.

ing interaction, B, is the corresponding delocalization energy due to the resonance, and is simply the quantum mechanical resonance energy (QMRE) of the transition state due to the delocalization of the four electrons over the three centers depicted in **3**. This description provides a physical mechanism for the barrier, in terms of the expression in eqn. (2), as a balance between the resonance-promoting distortion energy and the resulting QMRE due to delocalization.

$$\underbrace{[X\text{-----}R\text{-----}X]^-}_{4e^-}$$

3

The connection between the central barrier of the identity reaction and the distortion energy has been projected in a recent *ab initio* study[21] which has shown that the central barrier of the gas-phase reaction, $X:^- + CH_3X \rightarrow XCH_3 + :X^-$, correlates linearly with the corresponding deformation energy, ΔE_{def}, which is simply the difference between the energies of the CH_3X molecule in its transition state geometry relative to its ground state geometry (within the $X:^-/CH_3X$ ion–dipole complex). The correlation which covers X groups like H, F, Cl, OH, HS, CH_3O, CN, NC, and HCC is nevertheless remarkably linear ($r = 0.98$) and reads as in eqn. (3). It follows from eqn. (3) that the barrier

$$\Delta E^{\neq}(X:^-/CH_3X) = \Delta E_{def}(CH_3X) - (25.1 \pm 3.3 \text{ kcal mol}^{-1}) \quad (3)$$

derives from the deformation that is required to carry the CH_3X molecule to its transition state geometry, and that the interaction of $X:^-$ with the deformed molecule at the transition state is stabilizing and approximately constant.

The first conclusion indicates that the height of the crossing point, which is the destabilization energy of the reactants at the transition state, is dominated by the deformation energy of the molecule rather than by the exchange (overlap) repulsion between the closed shell $X:^-$ and CH_3X. The root cause of this trend can be deduced from Fig. 1 by reconsideration of the resonance, of the ground and charge-transfer states, under a frozen C–X bond distance $d°$, corresponding to the ground-state molecule. This distortion is schematized in the pictorial representation of **4** by the thick arrows which indicate the motions of the various atoms.

In scenario **4**, the only CH_3X deformation is the umbrella mode of the CH_3 angle that destabilizes the ground state

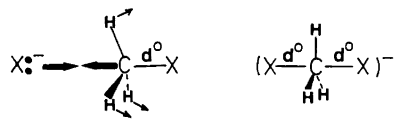

4 **5**

only slightly (18–40 kcal mol^{-1})[21] relative to the gap size. The same motion has a marginal effect on the energy of the charge transfer state (either slight destabilization or stabilization),[22] so that by mere flattening of the CH_3 group, the gap between the two states remains large. What reduces the gap is the large destabilization of the ground state, which is caused by the approach of $X:^-$ and CH_3X to the short $d°$ distance where their mutual closed-shell overlap repulsion is large. This additional destabilization of the ground state along with the bond-making stabilization of the charge-transfer state are responsible for the resonance between the two states. Thus, in the frozen C–X scenario (**4**) the ground state destabilization at the crossing point will be dominated by exchange (overlap) repulsion and not by the molecular deformation.

Clearly, if the frozen C–X scenario were a favourable option, all transition states would have been extremely compact with C–X lengths equal to the ground-state molecule, as depicted in **5**. However, since the CH_3 moiety is compact and has first row constituents, its overlap repulsion with the the closely distant $X:^-$ would be prohibitively large (e.g., ≥ 80 kcal mol^{-1} for $H:^-/CH_4$, $Cl:^-/CH_3Cl$, etc.) and would generate a very high crossing point. This high energy is avoided by activating the C–X stretching mechanism, because thereby $X:^-$ approaches CH_3X to a distance where the overlap repulsion is not severe and is counterbalanced by the electrostatic and polarization interactions (of $X:^-$ with CH_3X). The net effect of the activation of the stretching deformation is that in S_N2 transition states the height of the crossing point, ΔE_c, will usually be dominated by the CH_3X deformation energy, which itself is dominated by the stretching component.[21]

The second conclusion from eqn. (3) is that the avoided crossing interaction B (the QMRE) does not vary strongly with the nature of X, and may be used as a constant in qualitative considerations. This greatly simplifies the use of the curve crossing model because we need only understand the factors that govern the height of the crossing point in order to make predictions as regards variations in the central barriers, in the deformation energies and in the extents of bond stretching in the transition states.

Reactivity trends in the gas phase identity S_N2 reaction. The heigh of the crossing point is given in eqn. (2) as a fraction, f, of the vertical electron transfer energy gap that has to be overcome by the deformation. Accordingly, two factors control the height of the crossing point and they are schematized in Figs 2 and 3.[10,16,21]

The first factor is the vertical electron transfer energy gap. If we compare two reactions which differ only in their gaps as in Fig. 2, then achieving resonance with a large gap will require a high deformation energy and will result in a high barrier, and *vice versa* when the gap is small. Using thermochemical considerations,[10,16] it is possible to show that the variation of the electron transfer energy gap quantity is dominated by D_{C-X}, the bond energy of the CH_3X molecule; the stronger the bond, the larger the vertical

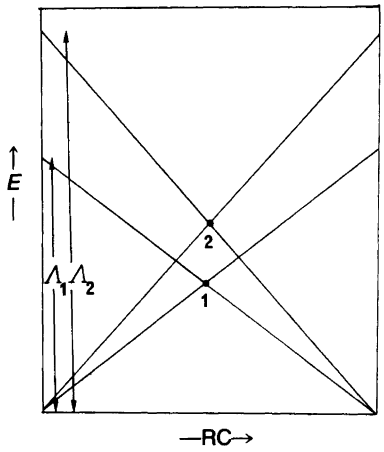

Fig. 2. A schematic description of the effect of the size of the vertical electron transfer energy gap (Λ) on the height of the crossing point. A small gap leads to a low-energy crossing point (1), while a large gap to a high-energy crossing point (2).

electron transfer energy gap. Thus for example, the C–X bond energy for X = halogen increases in the order $D_{C-F} > D_{C-Cl} > D_{C-Br} > D_{C-I}$, and the central barriers as well as the deformation energies vary in the very same order.[10,16,21]

The second factor that determines the height of the crossing point is f, which according to eqn. (2) is the fraction of the gap (Λ) that enters under the crossing point, i.e., $f = \Delta E_c/\Lambda$. If we compare reactions which have a *constant* gap, then the height of the crossing point will depend on the slope of the curves, as shown in Fig. 3. The slope (for a constant gap) depends, *inter alia*,[10] on how steeply the charge-transfer state descends owing to the bond-coupling interaction between the two odd electrons of X· and $(R\dot{:}X)^-$. If the odd electrons are *localized* on those atomic centers that eventually participate in the new

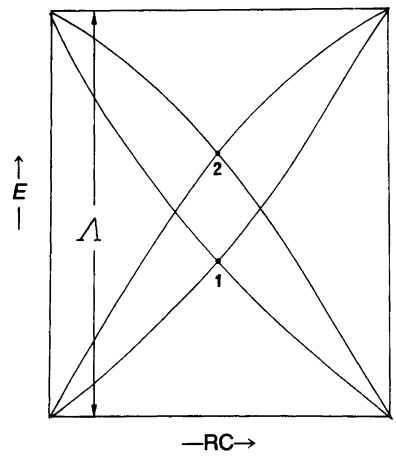

Fig. 3. A schematic description of the effect of the curve slopes on the height of the crossing point (for a given constant gap, Λ). Case 1 corresponds to a situation with localized odd electrons in the charge-transfer state. Case 2 corresponds to a situation with delocalized odd electrons in the charge-transfer states.

bond, then the strong bond coupling leads to a steep descent as in case 1. In comparison, if the odd electrons are *delocalized*, the weak bond coupling interaction leads to a shallow descent of the curves as in case 2 in Fig. 3. Thus, the size of f is larger the more extensive the delocalization properties of the X· and $(R\dot{:}X)^-$ species in the charge transfer state. Let us discuss therefore the delocalization properties of these species.

The radical anion $(R\dot{:}X)^-$ which possesses two σ electrons and one σ* electron (**1**) can be described in VB terms as a hybrid of two structures with weights, $W_{X:}$ and $W_{R:}$ as expressed by eqn. (4). An important property that governs

$$(R\dot{:}X)^- = (W_{X:})^{1/2}\,[R\cdot\ :X^-] \leftrightarrow (W_{R:})^{1/2}\,[R:^-\cdot X];\quad (W_{X:}) + (W_{R:}) = 1 \qquad (4)$$

$W_{R:}$ and $W_{X:}$ is the energy difference between the two VB structures, as schematized in their mixing diagram in Fig. 4. The energy difference is approximately the difference between the electron affinities of the X and R radicals ($A_{X\cdot} - A_{R\cdot}$). For a constant R (R = CH_3) this gap variation is determined by the electron affinity of X alone; a small $A_{X\cdot}$ leads to large $W_{R:}$ and vice versa. When $W_{R:}$ is large, the odd electron has a smaller probability of being on the reaction center R, and as a result the bond coupling interaction, between $(R\dot{:}X)^-$ and X·, becomes weak followed by a large f factor. These relationships can be expressed as

$$f \propto W_{R:} \propto 1/(A_{X\cdot} - A_{R\cdot})^2;\ A_{R\cdot} = \text{constant} \qquad (5)$$

in eqn. (5). Thus, X radicals that have low electron affinities are for example, H, NH_2, OH, CH_3O, SH and CH_3S. These groups will lead to radical anions with relatively large $W_{R:}$ and hence also a large f factor. On the other hand, halogen atoms have high electron affinities and will accordingly generate radical anions with small $W_{R:}$ and small f.[10,16,21]

According to Fig. 4, the $W_{R:}$ property is determined also by the interaction matrix element between the two VB structures. The matrix element is related to the binding ability of X, and very strong binders possess fairly large $W_{R:}$ in comparison with X groups which possess equal electron

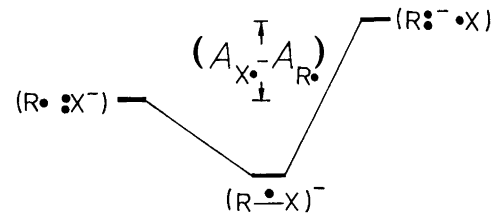

Fig. 4. An interaction diagram showing the mixing of the two VB structures, on the left- and right-hand sides, to generate the radical anion, in the center. According to perturbation theory, the mixing of $(R:^-\cdot X)$ into $(R\cdot\ :X^-)$ depends on their energy gap (given by the electron affinity difference $A_{X\cdot} - A_{R\cdot}$) and on their interaction matrix element (β_{RX}), by the following expression: $W_{R:} \sim (\beta_{RX}/A_{X\cdot} - A_{R\cdot})^2$.

Table 1. Curve crossing factors, deformation energies and central barriers for the gas phase reaction: $X^- + CH_3X \rightarrow XCH_3 + X^-$.

Entry	X^-	$(I_{X\cdot}^* - A_{RX}^*)^{a,b}$	$(W_{R\cdot})^b$	$(\Delta E_{def})^{a,c}$	$\Delta E^{\neq}$(*ab initio*)^{a,c}	$\Delta E^{\neq}$(exptl.)^{a,d}
1	F^-	135	0.242	40.8	11.7	ca. 19[e]
2	Cl^-	113	0.251	28.9	5.5	ca. 10; 13.2(2)[f]
3	HCC^-	145	0.362	72.5	50.4	ca. 41
4	HO^-	109	0.357	52.1	21.2	ca. 27
5	HS^-	95	0.340	38.8	15.6	ca. 24

[a]In kcal mol^{-1}. [b]From Refs. 10 and 21. [c]From Ref. 21. [d]From Ref. 17(a). [e]From Ref. 17(b). [f]From Ref. 17(c).

affinities, $A_{X\cdot}$, but are weaker binders (e.g., CCH and CN vs. I and Cl).

Other delocalization properties which lead to a high f factor are delocalization of the radical anion over a few identical C–X linkages as in CH_4^-, $CH_2Cl_2^-$, and so on.[10] Delocalization of the odd electron in $X\cdot$, as in $PhCH_2\cdot$, leads also to a larger f factor. These are the key, but not sole, determinants of the f factor, and there are other effects, a fuller discussion of which appears in a number of papers,[16] a review[10] and a forthcoming monograph.[23]

To summarize: delocalized odd electrons in the vertical charge-transfer state delay the bond-coupling interaction and cause the ground state to distort proportionally more in order to achieve resonance with the charge-transfer state. Thus, the f factor can be called *a bond-coupling delay index.*

Table 1 shows a few data which illustrate the interplay of the vertical electron transfer energy gap and the bond-coupling delay index. Thus, entries 1 and 2, and entries 3–5, form two groups, each possessing approximately constant $W_{R\cdot}$ and hence also constant f. As predicted above, in both groups both the barrier and the deformation energy increase as the vertical electron transfer energy gap increases. If, on the other hand, one wants to compare, for example, Cl^- in the first group to OH^- in the second group, the gap is now almost constant and both the barrier and the deformation energy increase in relation to the $W_{R\cdot}$ quantity. The two types of reactivity trends provide us the two aspects of the S_N2 reaction;[10,16,21] a transformation that involves simultaneously, a single electron 'movement' and bond coupling, or in short a single electron shift reaction as opposed to a SET reaction where the bond coupling is a separate event.

Fig. 5 shows a quantitative application of the model using the model expression of eqn. (6). Since f is proportional to

$$\Delta E^{\neq} = f(I_{X\cdot}^* - A_{RX}^*) - B; f = W_{R\cdot}, B = 14 \text{ kcal mol}^{-1} \quad (6)$$

$W_{R\cdot}$, and the latter values are in the range of algebraically reasonable f values,[10] it was decided simply to equate f with $W_{R\cdot}$. The value of B was then estimated from eqn. (6), by using a barrier value; $\Delta E^{\neq}$ for F^-/CH_3F 19 kcal mol^{-1},[16b] and carried over as a constant for all the reactions. It is seen from Fig. 5 that the model expression gives a reasonable correlation with the barriers estimated from experimental

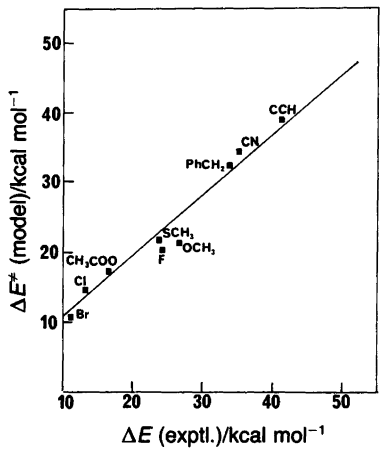

Fig. 5. A plot of model barriers [eqn. (6)] against the experimental gas-phase barriers derived by the RRKM procedure (Ref. 17) for the identity reaction of X^-/CH_3X. The various X groups are shown by the data points.

rate data by the RRKM procedure.[17] An equally good correlation is obtained if the model barriers are plotted against the *ab initio* computed barriers (by the 4-31G basis).[23] Thus, a semiquantitative analogue of the curve crossing diagram based on the interplay of donor–acceptor capabilities and bond-coupling effects captures the essence of the barrier problem.

Comments on the avoided crossing interaction in the identity S_N2 reaction. The value of B has a few interesting aspects. As discussed above, B is the quantum mechanical resonance energy (QMRE) of the transition state, and it reflects the stabilization energy that arises from the delocalization of the four electrons over the three centers, as depicted above in **3**. The value of 14 kcal mol^{-1}, espoused by eqn. (6) is close to a value of 15–16 kcal mol^{-1} which has been recently computed in a VB *ab initio* study of the curve crossing diagram for H^-/CH_4.[24] Incidentally, this value is also close to the resonance energy of allylic anions (14–18 kcal mol^{-1})[25] which are isoconjugate with the S_N2 transition state. Clearly, though the absolute value we use for B should be considered a rough estimate, it is still a reasonable one and it follows that the QMRE of the S_N2 transition state is a significant quantity which, in turn, reflects the substantial bond coupling in the transition state.

Another point is the apparent small dependence of the QMRE on the nature of X in the transition state. A physical basis for this emerges from a VB derivation[26] which shows that B should be proportional to the C–X bond strength in the transition state. Since the C–X bond in the transition state is weakened, the range of transition state bond energies is narrowed, leading thereby to a narrow range of QMRE values. We therefore do expect to find variations in the value of the QMRE as a function of X, but we also expect this variation to be narrower than the variation in the other reactivity factors which determine the magnitude of the deformation energy, i.e. the energy that is required to promote resonance between the ground and charge-transfer states.

Transition state geometries. Since the deformation that promotes the resonance between the ground and charge-transfer states is distinguished as the C–X stretching,[10,21] it is possible to discuss the geometry of the transition state in much the same manner as we discuss barriers. To unify the comparison between different transition states, we define the percentage bond stretching in the transition state relative to the ground state, in eqn. (7a) while the 'looseness' of the transition state is defined in eqn. (7b) as the sum of the percentage bond stretching for the left- (l) and right- (r) hand side C–X bonds in the transition state.

$$\%CX^{\neq} = 100\,(d^{\neq}_{CX} - d^{\circ}_{CX})/d^{\circ}_{CX} \qquad (7a)$$

$$\%L^{\neq} = (\%CX^{\neq})_l + (\%CX^{\neq})_r \qquad (7b)$$

Table 2 shows the curve-crossing factors alongside computed[21] looseness indexes of the respective transition states, and again two groups, each having a constant $W_{R:}$, can be distinguished in entires 1–3 and 4–6. It is seen that in each group, by itself, the looseness of the transition state increases as the vertical electron transfer energy gap increases. If however, we compare Cl^-, in the first group, with HO^-, in the second group, the gap is now approximately constant, and in accord with expectations the looseness increases as $W_{R:}$ becomes larger. It is apparent that transition state looseness behaves as do the corresponding barriers, and this may be witnessed from the comparison with the trends discussed by appeal to Table 1. Thus, both barriers and transition state geometries reflect the deformation energy that is required in order to destabilize the ground state and bring it into resonance with the charge-transfer state.

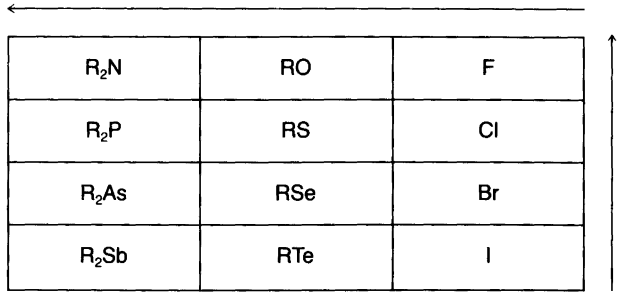

Fig. 6. A mini periodic table which summarizes reactivity patterns in $X^- + RX \rightarrow XR + X^-$. The various X groups are indicated in the table. The arrows point the directions in which both the barrier ($\Delta E^{\neq}$) and the looseness ($\%L^{\neq}$) of the transition state increase.

The mini periodic table of identity S_N2 reactivity and transition state structural trends. The foregoing discussions show that reactivity and transition state structure are determined by the interplay of the vertical electron transfer energy gap and the bond-coupling delay index ($W_{R:}$). We recall that the vertical electron transfer energy gap increases as the C–X bond energy (D_{C-X}) increases, and that $W_{R:}$ decreases as the electron affinity $A_{X\cdot}$ increases.[10] These simple thermochemical relationships provide us with a convenient means of organizing the reactivity patterns in the mini periodic table shown in Fig. 6, where the arrows indicate the directions in which both $\Delta E^{\neq}$ and $\%L^{\neq}$ increase. Thus up a column of our mini table, $A_{X\cdot}$ is almost constant while D_{C-X} increases rapidly. As a result both the barrier and the percentage transition state looseness should consequently increase up a column. On the other hand, on moving from right to left in a row of the mini table, the bond energy slowly decreases but $A_{X\cdot}$ decreases rapidly, and as a result it is expected that both the barrier and the looseness of the transition state will show a slow increase.

All the trends that are known to us about identity S_N2 reactions are in harmony with the predictions of the mini

Table 2. Curve crossing factors and looseness indexes for $(XCH_3X)^-$ transition states.

Entry	X^-	$(I_{X:}^* - A_{RX}^*)^a$	$(W_{R:})$	$\%L^{\neq}$(*ab initio*)^b	$\%L^{\neq}$(MNDO)^c
1	F^-	135	0.242	50.0	–
2	Cl^-	113	0.251	42.4	38
3	Br^-	99	0.246	–	35
4	HCC^-	145	0.362	90.0	–
5	HO^-	109	0.357	60.8	–
6	HS^-	95	0.340	56.8	–

[a] In kcal mol^{-1}. [b] From Ref. 21. [c] From Ref. 27(b).

periodic table of reactivity. Some of the predictions will await their test.

Identity S_N2 reactivity in solution. The avoided crossing diagram for a solution phase has a general form identical with the gas phase diagram (see the caption to Fig. 1).[10,27] The difference is that now the charge-transfer states are also vertical with respect to the orientations of the solvent molecules about the X· and $(R\text{-}X)^-$ species. This is indicated in the caption to Fig. 1 by the notation s* that signifies that the vertical charge-transfer states have the exact same solvent orientations as the corresponding ground states. Drawing **6** illustrates this situation, by reference to the solvated $X:^-(s)$ in the ground state and X·(s*) in the vertical charge-transfer state. The solvent molecules are schematized as arrow dipoles, merely for the sake of illustration, and have identical orientations about both $X:^-(s)$ and X·(s*). For $X:^-(s)$, in the ground state, these are equilibrium orientations that stabilize the charge, but for the neutral charge transfer species, X·(s*), these same orientations constitute a non-equilibrium arrangement.

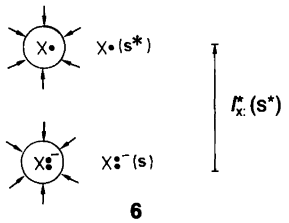

6

Thus, the vertical charge-transfer states in the avoided crossing diagram of Fig. 1 are characterized by a state of non-equilibrium solvation, and the reaction coordinate involves both molecular and solvent reorganizations.[10,27] This, in turn, means that the solvent is not a 'spectator' but has its own specific requirements to achieve the transition state, and not every superstructure which possesses a symmetric molecular structure $[X\text{---}CH_3\text{---}X]^-$ is a true transition state. In this respect the diagram in Fig. 1 is a narrow window in the multidimensional space for those crossing events which follow the constraints of symmetric solvent orientations and molecular structure in the transition state.

The vertical electron transfer energy gap in a solvent involves, in addition to the gas phase gap, a solvent reorganization energy term that reflects the state of non-equilibrium of the vertical charge-transfer species. The gap expression is eqn. (8), where ϱ is the solvent reorganization factor and $\Delta G_s(X:^-)$ is the solvation energy of the anion $X:^-$.[10,27] The reorganization factor itself is given by eqn. (9) as a function of the static (ε) and optical dielectric constants, the latter being simply the square of the refractive index (n^2). It is apparent from eqn. (8) that the solution-phase gap is larger than the gas-phase gap by a considerable amount, unless the factor ϱ is very small which is the case only for aromatic and hydrocarbon solvents.

$$[I_{X:}^* - A_{RX}^*](s^*) \sim [I_{X:}^* - A_{RX}^*](g) + 2\varrho|\Delta G_s(X:^-)|;\ \Delta G_s(X:^-)<0 \quad (8)$$

$$\varrho = (\varepsilon - n^2)/[n^2(\varepsilon - 1)] \quad (9)$$

The expression for the barrier is given, by analogy with the gas phase, by eqn. (10). The first term in the equation is

$$\Delta E^{\neq} = f[I_{X:}^* - A_{RX}^*](s^*) - B \quad (10)$$

the height of the crossing point which now constitutes the molecular deformation and solvent reorganization energies which are required to destabilize the ground state so that it achieves resonance with the charge transfer state, while the second term is the QMRE of the transition state due to the resonance of the four electrons across the three centers (**3**).

Table 3 shows the gaps and $W_{R:}(s^*)$ quantities in water and DMF as solvents, along with corresponding experimental and Marcus-equation-derived barriers.[18,19] The trends in the reactivity factors are seen to be almost identical with the gas-phase trends (Table 1), because the $W_{R:}(s^*)$ quantities are dominated by the intrinsic molecular properties (i.e., $D_{C\text{-}X}$ and $A_{X\cdot}$), while in the case of the vertical electron transfer energy gaps, the solvent-related terms vary in the same order as the intrinsic properties.[10,27] Con-

Table 3. Curve crossing factors and barriers for the reaction: $X^- + CH_3X \rightarrow XCH_3 + X^-$, in H_2O and DMF.

Entry	X^-	H_2O			DMF		
		Gap[a,b]	$W_{R:}(s^*)$[b]	$(\Delta E^{\neq})$[a,c]	Gap[a,b]	$W_{R:}(s^*)$[b]	$(\Delta E^{\neq})$[a,c]
1	F^-	259	0.206	31.8	230	0.208	–
2	Cl^-	204	0.239	26.6	181	0.243	22.7
3	Br^-	179	0.241	23.7	160	0.242	18.4
4	I^-	150	0.243	22.0	137	0.242	16.0
5	NC^-	242	0.304	50.9	218	0.304	–
6	HO^-	225	0.309	41.8	196	0.324	–
7	PhS^-	171	0.326	ca. 35[d]	152	0.328	–

[a]On kcal mol^{-1}. [b]Gap = $(I_{X:}^* - A_{RX}^*)(s^*)$ from Ref. 10. [c]From Ref. 18. See also Refs. 19 and 10. [d]Value in ethanol, from Ref. 19(a).

sequently, the trends in the barrier heights are identical, in the two solvents and in the gas phase. Moreover, as before there exists an interplay between the donor–acceptor controlled trend (entries 1–4, or 5–7) and the bond-coupling controlled trend (e.g., entry 3 vs. 7); reflecting together the single electron shift character of the transformation.

Solvent reorganization and molecular barriers. The total barrier in solution can be separated into two contributions, by use of eqns. (8) and (10). As shown in eqn. (11) the first term, inside the braces, involves the gas-phase electron transfer energy gap while the second term involves the solvent reorganization energy. These two contributions to the total barrier are shown separately in eqns. (12a) and (12b), and are identified as the molecular barrier, $\Delta E^{\neq}$(MOL), and the solvent reorganization barrier, $\Delta E^{\neq}$(SR).[10]

$$\Delta E^{\neq} \sim \{f[I_{X:}^{*} - A_{RX}^{*}](g) - B\} + 2f\varrho|\Delta G_s(X:^{-})| \quad (11)$$

$$\Delta E^{\neq}(MOL) = f[I_{X:}^{*} - A_{RX}^{*}](g) - B \quad (12a)$$

$$\Delta E^{\neq}(SR) = 2f\varrho|\Delta G_s(X:^{-})|;\ \Delta G_s(X:^{-})<0 \quad (12b)$$

The molecular barrier is the contribution of the molecular system that has to distort to establish the resonance between the 'bare' ground and vertical charge-transfer states. The solvent reorganization barrier, $\Delta E^{\neq}$(SR), refers to the reorganization effort of the solvent to respond to the switch of the charge which attends the resonance condition of the molecular system. There is an analogy between the solvent reorganization term in eqn. (12b) and the solvent reorganization barrier which attends an electron transfer process $X:^{-} + X^{\cdot} \rightarrow X^{\cdot} + X:^{-}$ in the Marcus–Hush theory of electron transfer.[28] The difference is that in the electron transfer barrier, $\Delta E^{\neq}$(SET), the f factor is replaced by the 1/4 factor. We recall that the f factor is the bond-coupling delay index of the molecular system, and the appearance of this factor in the solvent barrier in eqn. (12b) means that in S_N2 reactivity, the solvent reorganization is part of the reaction coordinate and coupled to the distortions and bond coupling motions of the molecular system.

This description of the solvent effect can be verified or falsified by studying the identity reactions in different solvents. A given reaction should exhibit, according to eqn. (11), a linear relationship between the barrier and the corresponding $|\varrho\Delta G_s(X:^{-})|$ quantity. The slope of this line should give, according to eqn. (11), the bond coupling quantity f which in turn, should vary in proportion to $W_{R:}(s^*)$ for different reactions.

Table 4 shows estimates of the molecular solvent barriers for a few solvents. These quantities are estimated by using $B = 14$ kcal mol^{-1} and $f = W_{R:}(s^*)$, much the same as above for the gas phase. It is seen that the solvent reorganization barriers are generally larger than the molecular barriers, but the latter are by no means negligible. The solvent reorganization barriers themselves diminish as the solvent reorganization factor, ϱ, decreases. Thus, in the case of benzene, where $\varrho = 0.0093$, the solvent barriers are almost zero. The solvent reorganization factor, ϱ, reflects the superstructure of the solvent. An organizable superstructure such as that in water possesses a large ϱ and requires substantial reorganization energy to respond to the charge switch. A small ϱ value reflects a fluxional superstructure that can respond more easily to the charge switch.[10,27]

Solvational effects in the transition state. The participation of the solvent orientational modes in the reaction coordinate has been emphasized by Bertràn and collaborators[29] who have shown that the reaction coordinate vector of the $[FCH_3F(H_2O)_2]^-$ transition state contains contributions from the motions of the water molecules. This necessarily means that equilibrium solvation cannot exist (in the statistical thermodynamic sense) with respect to the orientational modes of the solvent molecules. These non-equilibrium effects and the timescale differences of the various motions take on a dynamic expression which has been discussed recently in the reaction dynamics studies of the Cl^-/CH_3Cl reaction in aqueous solution.[30,31] Thus, Bergsma *et al.*[30] have shown that the transmission coefficient for this reaction at the D_{3h} 'molecular transition state' is 0.55, which in turn means that about half of the trajectories which reach the geometry of the *molecular* transition state are reflected back to the reactants. The successful trajectories are those that involve symmetrical solvent configurations about the molecular species.

The curve crossing diagram of Fig. 1 allows us to think about this dynamics effect of the non-unity transmission

Table 4. Molecular and solvent reorganization barriers for: $X^- + CH_3X \rightarrow XCH_3 + X^-$, in a number of solvents.

Entry	X^-	$\Delta E^{\neq}$(MOL)[a,b]	$\Delta E^{\neq}$(SR)[a,b]				
			H_2O[c]	MeOH[d]	DMF[e]	DMSO[f]	C_6H_6[g]
1	F^-	ca. 14	ca. 24	ca. 23	ca. 18	ca. 17	0.3
2	Cl^-	ca. 13	ca. 21	ca. 20	ca. 16	ca. 15	0.3
3	Br^-	ca. 10	ca. 19	ca. 18	ca. 14	ca. 14	0.2
4	I^-	ca. 6	ca. 17	ca. 16	ca. 14	ca. 13	0.2

[a] In kcal mol^{-1}. [b] Using eqn. (12a,b) and $f = W_{R:}(s^*)$. [c] $\varrho = 0.56$. [d] $\varrho = 0.55$. [e] $\varrho = 0.48$. [f] $\varrho = 0.45$. [g] $\varrho = 0.0093$.

coefficient, by considering the resonance condition of the ground and charge-transfer states under variety of distortion mechanisms. Imagine thus, X_l^-(s) and CH_3X_r(s) in the ground state (l,r stand for left and right) approaching each other along the Walden inversion trajectory that leads to the D_{3h} molecular structure. Because of the fact that the strongly oriented solvent molecules around X_l^-(s) are 'sticky' (or inertial), the reorganization of the solvent may lag behind the bonding changes of the molecular system. We may therefore consider the question of achieving the resonance condition along those reaction trajectories which are typified by largely frozen solvent configurations. In this scenario, the ground state will reach a symmetric D_{3h} molecular structure surrounded by solvent molecules which still largely retain their tight positions around X_l^- but not around X_r. At these same geometry and solvent orientations the charge-transfer state is still high in energy, due to the mismatch between the solvent orientations and the molecular charge (which is now primarily on X_r). It follows that the D_{3h} structure with the asymmetric solvent configurations does not lead to the requisite resonance between the ground and the charge-transfer states. In this case there is no avoided crossing, no transition state is achieved and the system simply relaxes back to the reactants; or in the molecular dynamics terminology[30] the D_{3h} structure is 'reflected' back to reactants. The condition for avoided crossing at the D_{3h} molecular structure is a symmetric solvent orientation, and these constrained structures are the true transition states.

It should be noted though that while the solvent orientations are symmetrized about the molecular charges of the transition state, this does not imply that there exists synchronicity of the molecular deformations and solvent reorganizational motions throughout the reaction trajectory. We have shown in the past that the various distortions are in any case not expected to be synchronized along the reaction coordinate (see, e.g., the discussion on pages 290–294 of Ref. 10). The exact details of the reaction coordinate are a matter of the match or mismatch between the timescales of the various movement types (the fast motion has to 'wait' for the evolution of the slow ones). Thus, a successful trajectory can be one in which the slow solvent fluctuation (from equilibrium positions around X_l^-/CH_3X_r) has to proceed to such an extent that it can drive and join the molecular system to the D_{3h} symmetrically solvated transition state. The opposite possibility also exists, that the molecular distortion is initially activated and subsequently drives the solvent to fluctuate to its final structure, and of course both movement types may sometimes be synchronized.[31] Thus, our analysis only means that a transition state is obtained where the two subsystems have both reached their requisite structures, but the movements need not be synchronized in every other section of the reaction coordinate.

The above non-equilibrium picture appears to be at variance with the physical organic view[32] that the solvent effect originates in the better solvation of the ground state relative to the transition state. In fact, as long as we do not insist that the solvation energy of the transition state is an equilibrium thermodynamic quantity, then the two pictures are qualitatively similar in a static sense. Thus, by use of eqns. (11) and (12), and by equating the molecular barrier to the gas-phase barrier, it is possible to derive an expression for the transition state solvation energy, ΔE_s $[(XCH_3X)^-]$, in eqn. (13), where we neglect the solvation of CH_3X in the ground state. It is seen that the equation

$$|\Delta E_s[(XCH_3X)^-]| = |\Delta G_s(X:^-)|\,(1 - 2\varrho f);\ f \propto W_{R:}^* \quad (13)$$

reaches the same conclusion as the physical organic approach, that the solvation energy of the transition state is smaller than the solvation energy of the corresponding ground state anion.[10,27]

Reactivity patterns in the non-identity S_N2 reaction

The curve crossing diagram for the non-identity reaction, eqn. (14), is shown in Fig 7. In discussing reactivity patterns according to the diagram, we have to consider now two different vertical electron transfer energy gaps (Λ), two slope factors (f), which involve two different bond-coupling delay factors due to the delocalization properties of the charge-transfer species, and the reaction ergonicity (ΔE) which reflects the relative stability of reactants and products (ΔE denotes general units: internal energy, enthalpy, free energy).[10]

$$Y:^- + R\text{–}X \rightarrow Y\text{–}R + :X^- \quad (14)$$

Though the reactivity patterns are now substantially more complex, the principle of activation does not change, and consists of deformations which are required to destabil-

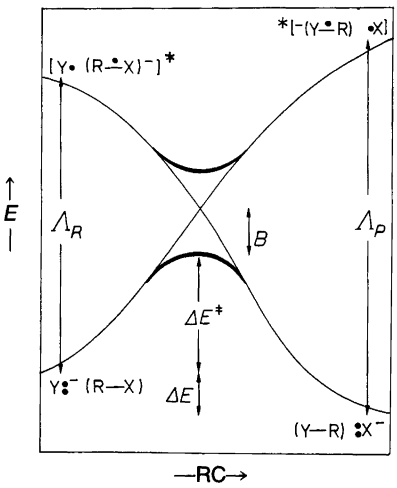

Fig. 7. A curve crossing diagram for a non-identity reaction. The gaps at the reactant and product extremes are $\Lambda_R = (I_{Y:}^* - A_{RX}^*)$ and $\Lambda_P = (I_{X:}^* - A_{RY}^*)$, and the corresponding slope factors of the curves are f_R and f_P.

ize the ground states, so they achieve resonance with the charge-transfer states. The reader is referred to a recent review[10] and a forthcoming monograph[23] for detailed analyses of specific problems, while here we attempt to draw some general features of the reactivity patterns.

The relationships between barriers and transition state geometries in non-identity reactions. A general feature which emerges from the consideration of the activation process is the relationship between barriers and transition state geometries. These relationships for the *ab initio* (the 4-31G basis set) data base are expressed in eqns. (15) and (16).[33] Eqn. (15) shows the correlation between the bond stretching percentages of the CH_3–X and CH_3–Y molecules and the barriers in the forward and reverse reactions, respectively. Eqn. (16) shows the relation between the sum of the percentages of bond cleavage for the two bonds in the transition state ($\%L^{\neq}$) against the sum of the forward and reverse barriers. The correlations are linear and cover a range of ca. 80% bond cleavage and 120 kcal mol^{-1} of barriers heights.[33]

$$\%CX^{\neq} = a\Delta E_f^{\neq} + b;\ a \sim 0.76\,(\text{kcal mol}^{-1})^{-1};\ b \sim 14 \quad (15a)$$

$$\%CY^{\neq} = a\Delta E_r^{\neq} + b \quad (15b)$$

$$\%L^{\neq} = \%CX^{\neq} + \%CY^{\neq} = a(\Delta E_f^{\neq} + \Delta E_r^{\neq}) + 2b \quad (16)$$

These relationships originate in the interplay of the curve crossing factors which determine the deformation energies that are required to overcome the vertical electron transfer energy gaps and achieve the resonance; large energy gaps and delocalized species in the charge-transfer states require high deformation energies, and hence also extensive bond stretchings. Recalling the properties which dominate the gaps and delocalization properties, we may summarize that, leaving groups X (or Y) which possess strong bonds and/or low electron affinities, $A_{X\cdot}$, are expected to possess high barriers and highly stretched C---X (or Y) bonds in the transition state.

The effect of the reaction ergonicity on the geometry of the transition state can be derived from eqns. (15a) and (15b), as shown in eqn. (17):[33] It is seen that the transition

$$\%CX^{\neq} - \%CY^{\neq} = a(\Delta E_f^{\neq} - \Delta E_r^{\neq}) = a\,\Delta E \quad (17)$$

state asymmetry, given by the difference in the bond stretching percentages in the transition state, correlates linearly with the reaction ergonicity. This relationship which is similar to the Leffler–Hammond postulate is valid despite the general invalidity of rate–equilibrium relationships for the same set of reactions (see the discussion below).[20,33]

Concepts: their breakdowns and irregular reactivity patterns in non-identity S_N2 reactions. The barrier in Fig. 7 is seen to be a function of five variables (if B is considered a constant). Regular reactivity patterns are therefore expected, as long as reaction series are considered in which the variation in one reactivity factor is not opposed by variations in the other factors. Breakdowns and irregularities are in turn expected whenever two or several reactivity factors vary in opposition.[10]

Some of the important concepts in physical organic chemistry are based on linear energy relationships between $\Delta E^{\neq}$ and ΔE. Thus, as long as ΔE is the dominant variation in a series of reactions, the series will obey rate–equilibrium relationships and their associated concepts, such as the reactivity–selectivity principle, the Bell–Evans–Polanyi principle, and so on. Multiple and opposing variations of the other reactivity factors will lead to breakdowns of these concepts. Examples of such breakdowns and other interesting reactivity patterns[10,16b] are discussed below and illustrate that the S_N2 reaction is usefully conceptualized as a single electron shift process.

Consider for example, the rate–equilibrium relationship in a gas phase series $X:^-/CH_3Cl$ where X is a halide.[10] In this series ΔE is the dominant reactivity factor, because the approximate constancy of $I_{X:}{}^*(g)$ for halides [here $I_{X:}{}^*(g) = A_{X\cdot}$] causes both the gap and the bond-coupling delay indexes to be approximately constant in the series. Rate–equilibrium relationships are consequently observed, and F^- that possesses the most exergonic reaction in the series leads to the smaller barrier in this series. However, if one compares for example, the gas-phase reactions of H^-/CH_3F ($\Delta E = -57$ kcal mol^{-1}) and F^-/CH_3Cl ($\Delta E = -28$ kcal mol^{-1}), then the more exergonic reaction possesses the larger barrier, because the effect of reaction ergonicity is counteracted by an opposite trend in the bond-coupling delay indexes.[10,16b] Breakdowns of of this nature of rate–equilibrium relationships are abundant among gas-phase S_N2 reactions.[10]

Interesting, in fact almost capricious, reactivity trends are reactivity crossovers and zigzags that occur because of opposing trends in the relative electron transfer energy gaps and slope factors (bond-coupling delay indexes or the bond interchange effects of the ΔE).[10,34] A typical example is the relative reactivity of two substrates toward a series of nucleophiles, when one of the substrates is a better electron acceptor than the second substrate but at the same time possessing a less favorable bond-coupling delay index. It is expected from the model, that initially at the low reactivity region, where barriers are high for both substrates, the substrate with the favorable bond-coupling delay index will react faster. As nucleophilic reactivity gradually increases, the better electron acceptor substrate is expected to gain superiority and react faster. Such reactivity crossovers and zigzags are observed, for example, in the relative reactivities of: $PhCOCH_2Br$ vs. $PhCH_2Br$,[35] p-$NO_2C_6H_4CH_2X$ vs. p-$CH_3OC_6H_4CH_2X$,[36] and $PhCOCH_2Br$ vs. CH_3I[37] toward a series of nucleophiles, or of $(CH_3)_3SiCH_2Cl$ vs. $CH_3CH_2CH_2Cl$[38] or C_2H_5Cl[39] toward different nucleophiles or toward the same nucleophile in different solvents.[38,39]

Reactivity crossovers reflect the single electron shift

character of the S_N2 process, as opposed to an actual SET process. In fact it can be generalized from the curve-crossing model that in comparisons of nucleophile–substrate pairs, where there exists a conflict between the trends in the electron transfer energy gap factor and the bond-coupling/interchange (i.e., slope) factors, the following reactivity pattern can be expected. Low reactivity regions tend to prefer higher reactivity of the reactant pair which possesses more favorable slope factors but which is a poorer donor–acceptor pair. However, regions of high reactivity tend to prefer the better donor–acceptor nucleophile–substrate pair. Reactivity crossovers may not always occur, but even then, the clash will be manifested as reactivity convergences.[10,34]

The dependence of 'nucleophilicity' on the reaction medium and substrate is another reactivity pattern which reflects the interplay of the electron transfer energy gap and slope factors. The case of the relative nucleophilicity of HO^- vs. CN^- is illustrative of this. In the gas phase OH^- is the better nucleophile,[32a,20b] because all of its reactivity factors, including the reaction ergonicity, are favorable relative to the CN^- (the ΔE values for the gas-phase reaction with CH_3Br are -54 and -35 kcal mol^{-1}, respectively). In solution phase S_N2, the nucleophilicity order is reversed[18] in favor of NC^-, because HO^- is much more strongly solvated than NC^- in any solvent and this renders the reactivity factors favorable for NC^- over HO^-. Thus, the stronger solvation of HO^- reduces the difference in the vertical ionization potentials and reverses the order of the reaction exoergicities; e.g., in aqueous solution[13a,b] $I^*_{HO:}(s^*) \sim 195$ kcal mol^{-1} and $I_{CN:}{}^*(s^*) \sim 200$ kcal mol^{-1}, and e.g., for $X:^+/CH_3Br$, the aqueous solution-reaction ergonicities[18] are $\Delta E(HO^-/CH_3Br) = -23$ kcal mol^{-1} and $\Delta E(NC^-/CH_3Br) = -37$ kcal mol^{-1}. Moving to better and better electron-acceptor substrates causes a gradual weakening of both NC–C and HO–C bonds, and this effect reduces in turn the reaction exoergicities, so that at some point HO^- can become once again the superior nucleophile due to its smaller vertical ionization potential. To the best of our knowledge this latter trend is observed occasionally with S_N2 substrates but mostly with very powerful electron-acceptor substrates such as the pyronin cation, and so on, where the relative nucleophilicity is $HO^- > NC^-$.[40] However, since the balance between the reactivity factors in solution is so delicate, we would not be surprised if it were found that the order of nucleophilicity of CN^- and HO^- exhibits crossovers and zigzags even with good acceptors. Nucleophilicity and its crossover patterns are then mere expressions of the single electron shift character of the nucleophilic–electrophilic reaction.

Indeed nucleophilicity can be capricious: it may follow either the relative vertical ionization potentials and obey the N^+ scale,[13a] or a mixture of ionization potential, bond strength and/or bond-coupling effects and obey more closely the Swain–Scott or the Edwards equations. Recent analyses of nucleophilicity[6,40] show that the redox potential $E°(Y·/Y:)$ by itself may occasionally serve as a useful nucleophilicity scale (Y: represents a nucleophile). Eberson has further demonstrated (pages 197–199 of Ref. 6) that the correlation between the redox potential and the Swain–Scott parameter, $n(CH_3I)$ holds over an extended range of both scales, but has significant local scatters. The $E°(Y·/Y:)$ quantity differs from the adiabatic ionization potential of the nucleophile by a constant,[40] and the adiabatic ionization potential itself differs, in turn, from the vertical ionization potential by the solvent reorganization energy.[13a,27] If we ignore this latter difference, then the correlation of $E°(Y·/Y:)$ with $n(CH_3I)$ and the local scatters represents the interplay of the single electron shift factors inherent in the S_N2 process. Clearly, according to the curve crossing diagram there cannot be a simple global nucleophilicity scale. Even for a given substrate such a nucleophilicity scale will require a multi-parameter equation which involves, at least, the vertical ionization potential of the nucleophile, the C–Y bond energy and the adiabatic ionization potential of the nucleophile (the last two quantities are constituents of the reaction ergonicity, ΔE). Since the vertical and adiabatic ionization potentials differ mainly[27] by the solvent reorganization energy, an alternative equation would include the solvent reorganization energy, associated with the vertical ionization process of Y:, the adiabatic ionization potential of Y:, and the C–Y bond energy. A simplification of the nucleophilicity scale can be achieved only if the property is inspected with "reaction families"[13a,b] where the various slope factors are together an effectively constant quantity. In these "reaction families" nucleophilicity is determined by the vertical ionization potential of the nucleophile.[13a,b]

The above examples serve as a demonstration of how complex reactivity patterns can be analyzed and predicted by a careful, though excruciatingly detailed, consideration of the electron transfer and bond-coupling/interchange reactivity factors.

S_N2 reactivity: concluding remarks. Much of what we know about S_N2 reactivity can be conceptualized in a unified manner by the curve-crossing modelling of the reaction, in Figs. 1 and 7. According to the model, the S_N2 reaction is a process which involves simultaneous single electron movement and bond coupling/interchange.[10–12] As such, the 'collage' of reactivity patterns can be conceptualized as the interplay of trends: those that reflect the the single electron switch aspect and follow the donor–acceptor capabilities of the reactants (vertical electron transfer energy gaps), and those which reflect the bond coupling and bond interchange aspects and depend on the delocalization properties of the charge transfer species and on the reaction ergonicity.

There are other aspects of S_N2 reactivity, such as the charge character of the transition state and the mechanistic spectrum that exists between S_N2 and S_N1, that can be conceptualized by the curve-crossing model. Suited to these purposes is the detailed approach[12] that considers explicitly each 'pure' VB configuration as a separate curve,

instead of the two curves with mixed VB character used in this review to conceptualize the barrier problem.

S_N2 and its competition with SET mechanisms

Aliphatic nucleophilic substitution has generally been thought to occur via the classical S_N2 or S_N1 mechanisms. However, recent experimental[1,6,15,41-44] work has modified this perception and added an alternative pathway to nucleophilic substitution, the SET mechanism which is described in eqn. (18).

$$Y:^- + R\text{–}X \rightarrow Y\cdot + (R\text{–}X)^- \rightarrow Y\cdot + R\cdot + :X^- \rightarrow Y\text{–}R + :X^- + \ldots \quad (18)$$

A well established SET mechanism is $S_{RN}1$ where the electron is transferred or 'photoinjected' into a π acceptor substituent or orbital of the substrate,[7] and in a subsequent step the electron is relayed, by π–σ^* avoided crossing[14,45] into the C–X bond of the substrate. The nature of the SET mechanism in aliphatic derivatives,[6,15,41-44] R–X, is much less well established. Firstly, simple alkyl derivatives do not possess a π-acceptor moiety which can initiate the electron acceptance, and secondly, though the experimental evidence for a SET pathway cannot be altogether dismissed, it is not as clear cut as in the $S_{RN}1$ mechanism.[15] Nonetheless, it is instructive to consider the case of aliphatic derivatives, because it is here where there exists a clear meeting ground between the single electron shift S_N2 mechanism and the single electron transfer SET mechanism.

Many of the features of the S_N2/SET dichotomy have already been analyzed and the theoretical[1,6,14] and experimental[6,7a,15] aspects have been reviewed. The following discussions are not intended to substitute detailed reviews of the field,[1,6] but primarily to provide a curve-crossing based general outline of the relationship between the S_N2 and SET mechanisms for reactions between 'electron-pair' nucleophiles ($Y:^-$) and R–X substrates having simple alkyl groups (radical-anion and odd-electron nucleophiles are not considered here, because their substituent/SET reactivity towards RX is a more complicated problem than even in electron nucleophiles. More details can be found in a recent paper.[46]

A curve crossing view of the relation between S_N2 and SET mechanisms. Consider a pair of reactants, $Y:^-$ and R–X which can undergo substitution by either S_N2 or SET mechanisms. Fig. 8 shows the curve crossing view for the S_N2 mechanism in part (a), and for the electron transfer step in part (b). The two mechanisms are seen to involve the avoided crossing of the same two states but along different reaction coordinates. In the S_N2 mechanism the resonance between the ground and charge-transfer states is promoted by a fully concerted distortion which also involves the solvent reorganizational modes [not specified in Fig. 8(a)]. In the SET mechanism, part (b) of Fig. 8, the resonance between the two states is achieved by a distortion which is

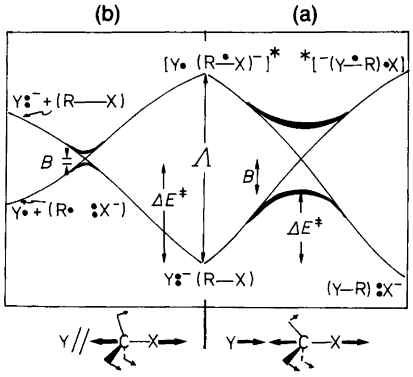

Fig. 8. Curve crossing diagrams showing the competition between the S_N2 [in (a)] and SET [in (b)] mechanisms in which a given $Y:^-$/RX pair can participate. The abscissa shows the reaction coordinate modes of the two mechanisms. Λ is the common vertical electron transfer energy gap for the two mechanisms. Note that $B(S_N2) >> B(SET)$, the latter being 'extremely small.'

devoid of the Y–C coupling, as indicated by the double slash, on the corresponding reaction coordinate. In this latter case the primary products are a radical, Y·, and an anion radical which may sometimes be extensively stretched,[6] and better described as a loose complex of R· and $X:^-$. The Y–C coupling, and hence the generation of the substituted product, will take place in subsequent steps which will be dominated by the dynamics of radical pairs in solution.[42,41e,47] This comparison of the two mechanisms also appears in the treatments of Walling[8] and Pross.[1] A somewhat related analysis of the SET mechanism has been described by Perrin.[48]

Fig. 8 views thus the two mechanisms as two competing or coexisting mechanisms driven by different distortion types. Indeed, the same equation, eqn. (19), can describe the barriers for both mechanisms, as a fraction of the vertical electron transfer energy gap minus the avoided crossing interaction, where f and B depend on the mechanistic choice of a given pair of reactants. Note that in eqn. (19) the effect of reaction ergonicity is implicity included in the f factor (see p. 215 of Ref. 10) which, in the absence of other adverse slope effects, becomes smaller the more exergonic the reaction.

$$\Delta E^{\neq}(S_N2/SET) = f(I_{Y:}{}^* - A_{RX}{}^*) - B \quad (19)$$

From the outset it is apparent that the lack of bond coupling puts the SET mechanism at a serious disadvantage in comparison with the S_N2 alternative. Nevertheless, a more extensive analysis of the quantities in eqn. (19) is required to provide insight into a few features of the SET/S_N2 dichotomy. Firstly, what is meant by a trajectory devoid of bond coupling? What does the transition state look like in the SET mechanism? When is it feasible to think about an actual S_N2/SET competition, and when do we have an either/or situation?

The avoided crossing interaction for SET and S_N2. Orbital symmetry considerations. The avoidance of bond coupling in the SET mechanism necessarily means a negligibly small B(SET), as opposed to a significant $B(S_N2)$. The stipulation of B(SET) $\rightarrow$ 0, which is also a feature of the Marcus theory of outer-sphere electron transfer,[6,28] puts a number constraints on the 'permitted' structures of the corresponding transition states. This section outlines structural types which meet the $B \rightarrow 0$ requirement.

In the first structural category we consider a backside attack, for which we can derive a general VB expression for B in terms of resonance integrals, β, orbital energies, e, and overlaps, s, for the appropriate fragment orbitals of the Y, R and X fragments, as shown in eqn. (20).[26] It is seen that B

$$B = C[\beta_{YR}s_{RX} + \beta_{RX}s_{YR} - (e_X + e_Y + e_R)s_{YR}\,s_{RX}];$$
$$C = -4/(1-s_{YR}\,s_{RX}) \qquad (20)$$

depends on the orbital overlap product $s_{YR}s_{RX}$, and will vanish whenever one of the overlaps or both become zero. Accordingly, among the possibilities that can lead to B(SET) $\rightarrow$ 0 are the structures where the Y---R distance is very long, or where the Y---R overlap vanishes by symmetry. We may therefore consider the S_N2/SET dichotomy as the outcome of maximization/minimization of the Y---RX orbital interactions.

The possibility of zero overlap due to large distance may not be a realistic sistuation, if the nucleophile is a free ion, because one would reasonably expect the reactants to form some sort of encounter complex in which the nucleophile nestles at the back of the carbon site of attack.[49] However, when the nucleophile is an ion pair, the positive counterion can separate the nucleophile and the substrate[50] as shown in **7** and keep them sufficiently far apart and disoriented to prevent bond coupling and lead to a transition state with B ~ 0. Of course the transition state will be generated from **7** as shown in **8** by deformation of the molecule, C–X stretching and umbrella motion, which induce the resonance between the ground and charge-transfer states, and thereby permit the occurrence of the SET step.

Orbital symmetry considerations provide a convenient search strategy for transition states which meet the zero B(SET) requirement in the backside attack. The general condition is a zero overlap between the HOMO of the nucleophile and the p-AO of the carbon site of attack. In a strict sense this will necessarily mean that the ground and the charge-transfer states, at the crossing point, possess different symmetries so that their crossing will not be avoided, i.e., B = 0. Specific types can be envisaged when the nucleophile has a delocalized electronic system as in fluorenide,[43] allyl anion,[44] and the enolate anion of 4-methoxycarbonyl-1-methyl-1,4-dihydropyridine.[41] In all these cases the HOMO of the nucleophile possesses antibonding regions which lead to a vanishingly small overlap with the p-AO of the carbon in R–X. In **9** is illustrated such an SET orientation alongside its normal S_N2 orientation in **10**, using the five-membered ring portion of a fluorenide anion. It is seen that the overlap with the p-AO of carbon is small in **9** and maximized in **10**. Thus, the S_N2 and SET mechanisms can in principle possess structurally similar transition states which maximize and minimize, respectively, the HOMO (Y) – p(carbon) overlap by reorientation of the nucleophile with respect to the carbon site of R–X. There may exist of course, in the same nucleophile, a few different molecular regions with antibonding character in the HOMO, all of which may be considered in a similar fashion to **9**.

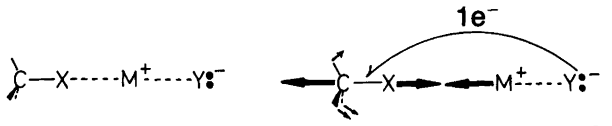

7 **8**

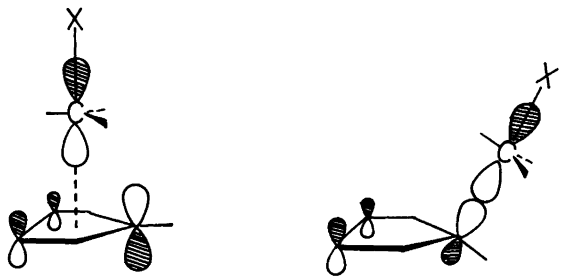

(*B*~0) (*B*>>0)

9 **10**

In the second structural category we may consider a frontside attack as a solution to the B(SET) $\rightarrow$ 0 requirement, as opposed to the backside S_N2 attack. In this case more insight may be gained by looking at the semidelocalized representation of the charge-transfer state in **1** in terms of the fragment orbitals φ_Y, σ_{CX} and σ^*_{CX}. The Y–C bond coupling and the avoided crossing interaction at the transition state depend on the φ_Y- σ^*_{CX} (HOMO–LUMO) overlap, which is close to zero in a frontside approach as illustrated in **11**.

11

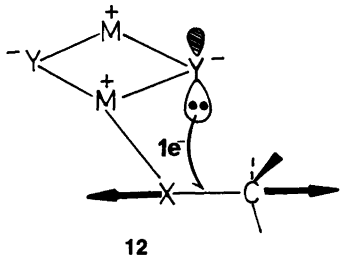

12

Frontside attacks may be the default option for substitution reactions of cases like adamantyl, or bornyl substrates[7a,41e] where the backside is blocked. The same result may be effected when the backside of the substrate is encumbered by steric effects and a frontside SET can be initiated from a complex in which the nucleophile is coordinated to the β hydrogen of the substrate. Similarly, when the nucleophile is a part of an ion-pairing aggregate, e.g., $(Li^+Y^-)_n$, where $n \geq 2$, the positive ion also coordinates the substrate, in such a fashion that within the aggregate complex a frontside attack is constrained (see **12**), while, as pointed out by Seebach,[51] the backside attack for the S_N2 reaction is possible only in an intermolecular fashion.

The orientational issue in SET reactions has been considered before by Lund,[41c] Bordwell *et al.*,[43] Welvart and collaborators,[52] Chanon and collaborators,[47a] Eberson (see Chap. V of Ref. 6), and by Savéant and collaborators.[53] The role of the HOMO–LUMO interaction has been discussed by Lund and Lund.[41d]

As discussed for the S_N2 sections, the magnitude of $B(S_N2)$ is in the order of 14 kcal mol^{-1}. It is very clear therefore that the B effect makes the SET mechanism intrinsically less favored than the S_N2 alternative, and the above structures for SET transition states are either default options or occurring as non-overlapping backside trajectories in some cases which are truly competitive with S_N2. In the following sections we discuss the factors which can make the SET mechanism competitive with its S_N2 alternative, for a given pair of reactants.

The S_N2/SET dichotomy: consideration of the distortion mechanisms. We recall, with reference to Fig. 8, that transition states are achieved by distortions which overcome the vertical electron transfer energy gap and promote resonance between the ground and charge-transfer states. Since every distortion destabilizes the ground state, we must search for distortions that most efficiently stabilize the charge-transfer state, $Y\cdot/(R\text{-}X)^-$. A pure umbrella opening of the valence angles about R confers approximately 0–5 kcal mol^{-1} of stabilization to the radical anion. A distortion of the radical anion, combining umbrella and stretch modes, does much better and confers stabilization energies in the range 20–50 kcal mol^{-1},[10] e.g., ca. 39 kcal mol^{-1} for $(CH_3\text{-}Cl)^-$.[54] Solvent reorganization by itself has about the same effect, of 30–50 kcal mol^{-1} of stabilization energy for each one of the species in the vertical charge-transfer state (recall that the solvent reorganization term is given by $\varrho\Delta G_s$, where the ΔG_s term is the solvation energy of the corresponding anion).[10] In comparison with these partial distortions, the complete S_N2 distortion, **2**, along with its associated solvent reorganization, stabilize the vertical charge-transfer states by as much as 150–250 kcal mol^{-1}, and this high efficiency is contributed by the bond coupling component of the distortion.

In conclusion, the efficiency of the distortions to promote resonance increases in the following order, complete distortion > solvent reorganization > C–X stretching >> bending distortion. This order provides us with a rough guideline for discussing the S_N2/SET competition because this competition depends on the feasibility of achieving resonance with a partial distortion devoid of bond coupling. Below we discuss the various factors in order, with reference to the barrier expression in eqn. (19).

The role of the vertical electron transfer energy gap in the S_N2/SET competition. The larger the vertical electron transfer energy gap, the more drastic a distortion is required to achieve the resonance. Thus, a large gap for a given $Y:^-$/R–X pair will require complete distortion and will lead exclusively to substitution via the S_N2 mechanism. Small gaps, on the other hand, may also be overcome by partial distortions and allow, under certain conditions (specified later), the stepwise SET mechanism to be competitive with its S_N2 alternative. Thus, if we arbitrarily take a barrier of ca. 25 kcal mol^{-1} as a limit of a feasibly fast SET reaction this will correspond to a benchmark value of 100 kcal mol^{-1} for the gap [using a reasonable set of values in eqn. (19), $f \geq 0.25$ and $B \sim 0$, as in the Marcus equation]. A larger value of the gap will allow us to rule out those poor donor–acceptor $Y:^-$/R–X combinations in which it is either impossible or too costly to achieve resonance by partial distortions. The factors which determine the gap size are qulitatively sketched below.

(a) The vertical ionization potential of the nucleophile ($Y:^-$) is given by eqn. (21):[10,13a,b;27] A small vertical ionization potential of the nucleophile requires low gas-phase ionization energies along with relatively small solvation energies, $[\Delta G_s(Y:)]$, and solvents which possess small reorganization factors ϱ. Suitable nucleophiles are, for example,[6,15,41-44] $R_2N:^-$, $R_2P:^-$, $R_3Sn:^-$, $R:^-$, and aggregates as $(R:^-\ Li^+)_n$ which have recently been shown by Renaud and Fox[55] to possess smaller oxidation potentials than their monomeric forms. The contribution of the solvent to the vertical ionization potential is given by the second term in eqn. (21) and can range between ≥ 100 kcal mol^{-1} in hydroxylic solvents down to ≤ 50 kcal mol^{-1} in non-polar solvents ($\varrho \sim 0.56 \rightarrow 0.009$).

$$I_{Y:}^*(s^*) \sim I_{Y:}^*(g) + |(1+\varrho)\Delta G_s(Y:)| \qquad (21)$$

(b) The vertical electron affinity of the substrate is given by eqn. (22):[10,13a,b;27] As a general rule, σ bonds are poor acceptors and A_{RX}^* (g) is normally a negative quantity which becomes less negative, and occasionally positive, due to the solvent effect which improves the vertical electron affinity.[10,27] For a given R group, the vertical electron affinity A_{RX}^* (g) increases, the weaker the R–X bond and the higher the X electron affinity.[10] Bond-weakening substituents on R, such as Ph and alkyl groups, improve the electron affinity of R–X. Electron-withdrawing groups on R increase the RX electron affinity as for example in CCl_4,

$$A_{RX}^*(s^*) \sim A_{RX}^*(g) + |(1-\varrho)\Delta G_s[(R\text{-}X)^-]| \qquad (22)$$

CF_3I, CF_3CH_2I, and so on.[10] It is then expected, that for a given R the highest vertical electron affinities will be of RI and RBr.[10]

The vertical electron transfer energy gap is obtained by the combination of eqns. (21) and (22) and is expressed according to eqn. (23). Using a range of ϱ values[10,27] and

$$[I_{Y:}^* - A_{RX}^*](s^*) \sim [I_{Y:}^* - A_{RX}^*](g) + |(1+\varrho)\Delta G_s(Y:)| - |(1-\varrho)\Delta G_s[(R\div X)^-]| \quad (23)$$

solvation free energies of anions[10,27,40] and radical anions,[56] in solvents with polarities between those of DMF and ethers, the solvent-related terms in eqn. (23) can be estimated to be in the range of 50–70 kcal mol^{-1}. Using this range of values, and the benchmark value of ≤ 100 kcal mol^{-1} for $[I_{Y:}^* - A_{RX}^*](s^*)$ we can estimate a range for the limiting values of the gas-phase vertical electron transfer energy gap, beyond which the SET mechanism in solution is expected to be exceedingly slow. This range is given in eqn. (24) which, despite the roughness of the estimation process, is seen to put a severe restriction on the feasible outer-sphere SET reactions for $Y:^-$/RX combinations (for a similar conclusion see Ref. 6 pp. 197–199).

$$[I_{Y:}^* - A_{RX}^*](g) \leq 30\text{–}50 \text{ kcal mol}^{-1} \quad (24)$$

The role of the bond-coupling/intercharge factors in the S_N2/SET competition. The slopes of the intersecting curves [f in eqn. (19)] have a dominant influence on the S_N2/SET competition. Because of the reaction ergonicity effect, the f factor for the S_N2 process is at the outset smaller than the corresponding f for the SET process. This, added to the effect of the avoided crossing B factor, normally gives an overwhelming superiority to the S_N2 process. However, whenever there exist slope effects which delay the bond coupling between the nucleophile and the substrate, the normal advantage of the S_N2 is counterbalanced, and the SET mechanism will become competitive and even prevail. Two slope factors are electronic delocalization effects and steric effects, as discussed below.

(a) *Delocalization effects.* Delocalization of the odd electrons in the charge-transfer state causes a shallow descent of the charge-transfer state and leads to a high barrier for the S_N2 mechanism.On the other hand, since the SET mechanism occurs along a reaction coordinate devoid of bond coupling, the odd electron delocalization will not exert its adverse influence on the descent of the charge-transfer state [hence a smaller f in eqn. (19)]. Examples of such delocalization effects are provided by substrates such as CBr_4[57] (which has a delocalized and stable radical anion), delocalized nucleophiles as the enolate derivative used by Lund,[41] and the fluorenide/CF_3CH_2–I combination which has been used by Bordwell and collaborators.[43]

(b) *Steric factors.* When the backside of R–X or the nucleophilic center are encumbered, the charge-transfer state descends in a shallow manner along the S_N2 coordinate but not so along the SET coordinate which is devoid of bond coupling. Examples of such steric effects are cases like t-Bu–X, neopentyl–X, or cases where the backside is completely blocked as in adamantyl–X,[7a,41] or when the backside blocking act is caused by coordination in an aggregate[51,58] as in **12**, or by a single counterion as in **7**.

Clearly, the combination of delocalization and steric effects is a good recipe for inducing SET propensity in a $Y:^-$/RX reactant pair.[1,41,43,53]

An application: transition state structure in SET reactions. Using the curve crossing guidelines in eqns. (19) and (21)–(24) and the $B \sim 0$ requirement, it is possible to make some educated deductions about barriers and transition state structures of SET reactions. As an example we consider the putative SET reaction between allyl anion (or a derivative of it) and t-Bu–I in the gas phase. The vertical electron transfer energy gap, in the gas phase, is very small: of the order of 10–20 kcal mol^{-1}.[10] An umbrella distortion coupled with a slight stretching of the C–I bond and with a slight angular deformation of the allyl anion will suffice, without a need for bond coupling between the reactants, to bring the ground and charge-transfer states into resonance. Since we need not consider the electron delocalization effect on the bond coupling, the f factor in eqn. (19) can be taken as ca. 0.25, as in the Marcus theory, and consequently the height of the crossing point will be 2.5–4 kcal mol^{-1} above the reactants. Using the expressions for the solvent effect in eqns. (21)–(22), it is possible to make a further rough estimate of a barrier of 15–17 kcal mol^{-1} in a solvent such as THF (ϱ ~ 0.43, $\Delta G_s \sim -60$ kcal mol^{-1}), certainly a feasible reaction. A more polar solvent will slow down the reaction, and a solvent such as DMF with a ϱ value of 0.48 will increase the barrier by ≥ 2 kcal mol^{-1}, but still a feasible reaction is expected. The root cause of this feasible SET reaction is the tiny vertical electron transfer energy gas-phase gap, which is well below the critical value derived from eqn. (24).

Simple models of curve crossing[10,26] can also provide rough geometric features for the t-Bu–I species at the crossing point, while the requirement for $B \sim 0$ will set the constraints on the permitted structural types that are SET and not S_N2 transition states. Two possible transition states are illustrated as **13** and **14** and both show that the substrate moiety is only slightly perturbed relative to the ground state molecule (d°_{CI} = 2.12 Å). In **13** we consider an allyl moiety, which occupies a backside position that is distant enough to avoid steric repulsion and, by virtue of orbital symmetry, maintains $B \sim 0$. An expected slight breaking of the symmetry, e.g., by a small angle recline of the allyl moiety, will induce a small avoided crossing interaction B. This transition state will resemble its S_N2 counterpart with the exception that in the S_N2 transition state the allyl moiety will be much closer to the t-Bu (ca. 2.2 Å) and coupled to the carbon site through one of the terminal allylic carbons. In **14**, we consider an alternative transition state, where the allyl moiety is segregated from the t-Bu

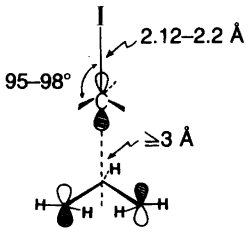

13

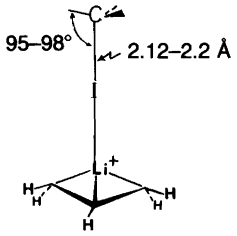

14

group by an Li^+ ion (e.g., if such ions are present in the solution phase reaction). The latter SET transition state obeys the $B \sim 0$ requirement and is structurally dissimilar to its S_N2 kin.

From an electronic point of view, the SET transition state is a resonating mixture similar to the S_N2 transition state, i.e., $Y:^-/R–X \leftrightarrow Y\cdot/(R\dot{-}X)^-$, but with high diradicaloid character, because of the small bond coupling. At the limit of zero bond coupling, as in **13**, the resonating structures may differ by symmetry and mix by breaking the symmetry. In **14** the mixing is assisted via delocalization through the metal ion. In certain cases, especially in the frontside attack, the triplet spin state of $Y\cdot/(R\dot{-}X)^-$ may well be lower than the singlet spin state. In this latter case the VB structures can mix mainly by spin–orbit coupling.[59] The corresponding SET 'transition state' will possess then mixed singlet–triplet character, and the reaction rate will be subject to acceleration by heavy atoms solvents, and to magnetic field effects.

The SET mechanism: concluding remarks. The avoided crossing model shows some expected general features of the SET mechanism. The establishment of these features will require the combined effort of experiment and theory.

The first and most challenging problem is to be able to characterize the structure of SET transition states. A possible strategy is the experimental derivation of the B values for SET reactions along recently discussed lines.[13a,b] Experimentally determined B values will provide at least an indication as to whether the SET transition states really approach the outer-sphere limit as is usually stipulated. In parallel, quantum mechanical computations at the MCSCF level can be used to locate and characterize SET transition states and compare them to the various archetypes discussed in this paper. Yet another line is to investigate electron transfer in rigid systems which include both the nucleophile ($Y:^-$) and the substrate (RX), but which preclude their coupling and substitution reaction. Such systems can provide a means of studying structure–reactivity relationships as well as isotope effects which, in turn, may be helpful in the deduction of the distortions that are required to achieve the SET transition states.

The second major problem, in our view, is to ascertain the role of ion pairing and ion-paired aggregates which seem to play an important role in making the SET mechanism feasible, as discussed by Seebach,[58] by Fox,[55] and in the present paper. A related problem which is not discussed here is the possible role of microassemblies of the substrates, $(RX)_n$, which can accept the electron and propagate it in a manner similar to the mechanism of conductivity or to the electron transfer relay mechanism proposed for the photosynthetic site.[60]

Finally, another point which we have not discussed and which requires detailed examination is the nature of the primary products of the electron transfer step (a radical and a radical anion or two radicals and an anion, $X:^-$), and the dynamics of and the governing factors in the subsequent steps of the SET mechanism. Some of these aspects have been addressed already by workers in the field.[6,15,41,42]

Summary

A 'movement' of a single electron is the basic and perhaps exclusive electronic reorganization that can take place between a nucleophile ($Y:^-$) and a substrate (R–X). This electronic event involves activation due to the distortions and solvent reorganizational modes that are required to overcome the vertical electron transfer energy gap and bring the ground and charge-transfer states into resonance (Fig. 8). The resonance condition can be achieved by a 'complete' distortion (**2**) which involves an umbrella inversion, C–X cleavage, Y–C bond coupling, and solvent reorganizational modes. This is the synchronous S_N2 or single electron shift mechanism. Alternatively, the resonance condition can be achieved by a distortion that is devoid of bond coupling. This is the single electron transfer (SET) mechanism, in which the electron transfer step precedes the bond-coupling step. Thus, the two mechanisms are electronically related and their transition states are structurally isomeric.

This review shows that the curve crossing model provides a unified insight into the reactivity patterns in the two mechanisms. Application to other reactions involving electrophile–nucleophile combinations is quite straightforward.[13a,b;46,61]

Acknowledgements. I am thankful to the following collaborators and friends for their contributions and inspiration in the course of the work on organic-chemical reactivity: E. Buncel, P. C. Hiberty, J. M. Lefour, G. Ohanessian, A. Pross, H. B. Schlegel, G. Sini, I. H. Um and S. Wolfe. Correspondence with J. F. Bunnett on the S_N2/SET dichotomy, after the 1985 Electron Transfer symposium in Carbondale, was illuminating.

References

1. Pross, A. *Acc. Chem. Res. 18* (1985) 212.
2. (a) Bank, S. and Noyd, D. A. *J. Am. Chem. Soc. 95* (1973) 8303; (b) Noyd, D. *Ph. D. Thesis,* State University of New York, Albany, N.Y. 1972.
3. Kochi, J. K. *Angew. Chem., Int. Ed. Engl. 27* (1988) 1227.
4. (a) Arnett, E. M., Molter, K. E., Marchot, E. C., Donovan, W. H. and Smith, P. *J. Am. Chem. Soc. 109* (1987) 3788; (b)

Guthrie, R. D. *J. Am. Chem. Soc. 91* (1969) 6201; (c) Han, C.-C. and Brauman, J. I. *J. Am. Chem. Soc. 110* (1988) 4048; (d) Verhoeven, J. W., Gersheim, W. V., Martens, F. M. and van der Kerk, S. M. *Tetrahedron, 42* (1986) 975.
5. (a) Chanon, M. *Bull. Chim. Soc. Fr. II* (1982) 213; (b) Burdett, J. K. *Comments Inorg. Chem. 1* (1981) 85; (c) Taube, H. *J. Chem. Educ. 45* (1964) 452.
6. Eberson, L. *Electron Transfer Reactions in Organic Chemistry*, Springer Verlag, Berlin–Heidelberg 1987.
7. (a) Rossie, A., Pierini, A. B., Palacios, S. M. *Adv. Free Radical Chem. In press*; (b) Bunnett, J. F. *Acc. Chem. Res. 11* (1978) 164; (c) Kornblum, N. *Angew. Chem., Int. Ed. Engl. 14* (1975) 734; (d) Russell, G. A. and Dannen, W. C. *J. Am. Chem. Soc. 88* (1966) 5663.
8. Walling, C. *J. Am. Chem. Soc. 102* (1980) 6854.
9. Shaik, S. S. *J. Am. Chem. Soc. 103* (1981) 3692.
10. Shaik, S. S. *Prog. Phys. Org. Chem. 15* (1985) 197.
11. Pross, A. *Adv. Phys. Org. Chem. 21* (1985) 99.
12. Pross, A. and Shaik, S. S. *Acc. Chem. Res. 16* (1983) 363.
13. (a) Shaik, S. S. *J. Org. Chem. 52* (1987) 1563; (b) Buncel, E., Shaik, S. S., Um, I. H. and Wolfe, S. *J. Am. Chem. Soc. 110* (1988) 1275; (c) Pross, A. *Isr. J. Chem. 26* (1985) 390; (d) Cohen, D., Bar, R. and Shaik, S. S. *J. Am. Chem. Soc. 108* (1986) 231.
14. Ref. 10, p. 306.
15. (a) Newcomb, M. and Curran, D. P. *Acc. Chem. Res. 21* (1988) 206; (b) Ashly, E. C. *Acc. Chem. Res. 21* (1988) 414.
16. (a) Shaik, S. S. *New J. Chem. 6* (1982) 159; (b) Shaik, S. S. and Pross, A. *J. Am. Chem. Soc. 104* (1982) 2708.
17. (a) Pellerite, M. J. and Braumann, J. I. *J. Am. Chem. Soc. 105* (1983) 2672; (b) Dodd, A. and Brauman, J. I. *J. Am. Chem. Soc. 106* (1984) 5356; (c) Barlow, S. E., van Doren, J. M. and Bierbaum, V. M. *J. Am. Chem. Soc. 110* (1988) 7240.
18. Albery, W. J. and Kreevoy, M. M. *Adv. Phys. Org. Chem. 16* (1978) 87.
19. (a) Lewis, E. S., McLaughlin, M. L. and Douglas, T. A. In: Harris, J. M. and McManus, S. P., Eds., *Nucleophilicity*, American Chemical Society, Washington DC 1987; (b) Lewis, E. S., Yousaf, T. I. and Douglas, T. A. *J. Am. Chem. Soc. 109* (1987) 2152.
20. (a) Wolfe, S., Mitchell, D. J. and Schlegel, H. B. *J. Am. Chem. Soc. 103* (1981) 7694; (b) Mitchell, D. J. *Ph. D. Thesis*, Queen's University, Kingston, Ontario, Canada 1981.
21. Mitchell, D. J., Schlegel, H. B., Shaik, S. S. and Wolfe, S. *Can. J. Chem. 63* (1985) 1642.
22. Cohen, D. and Shaik, S. S. Unpublished *ab initio* studies of radical anions with different basis sets and at different levels of sophistication.
23. Shaik, S. S., Schlegel, H. B. and Wolfe, S. *Theoretical Physical Organic Chemistry. Application to the S_N2 Transition State*, Wiley Interscience, New York. *To be published.*
24. Sini, G., Shaik, S. S., Ohanessian, G., Lefour, J. M. and Hiberty, P. C. *J. Phys. Chem. 93* (1989) 5661.
25. Farnham, W. B., Middleton, W. J., Fultz, W. C. and Smart, B. E. *J. Am. Chem. Soc. 108* (1986) 3125.
26. Shaik, S. S. In: Bertrán, J. and Csizmadia, I. G., Eds., *New Theoretical Concepts for Understanding Organic Reactions*, NATO ASI Series, Kluwer Academic Publishers, Dordrecht 1989.
27. (a) Shaik, S. S. *J. Am. Chem. Soc. 106* (1984) 1227; (b) Shaik, S. S. *Isr. J. Chem. 26* (1985) 367.
28. (a) Marcus, R. A. *Annu. Rev. Phys. Chem. 15* (1964) 155; (b) Hush, N. S. *Trans. Faraday Soc. 57* (1961) 557.
29. Bertrán, J. In: Bertrán, J. and Csizmadia, I. G., Eds., *New Theoretical Concepts for Understanding Organic Reactions*, NATO ASI Series, Kluwer Academic Publishers, Dordrecht 1989.
30. (a) Bergsma, J. P., Gertner, B. J., Wilson, K. R. and Hynes, J. T. *J. Chem. Phys. 86* (1987) 1356; (b) Gertner, B. J., Bergsma, J. P., Wilson, K. R., Lee, S. and Hynes, J. T. *J. Chem. Phys. 86* (1987) 1377.
31. Hwang, J.-K., King, G., Creighton, S. and Warshel, A. *J. Am. Chem. Soc. 110* (1988) 5297.
32. (a) Olmstead, W. N. and Brauman, J. I. *J. Am. Chem. Soc. 99* (1977) 4219; (b) Chandrasekhar, J., Smith, S. F. and Jorgensen, W. L. *J. Am. Chem. Soc. 107* (1985) 154.
33. Shaik, S. S., Schlegel, H. B. and Wolfe, S. *J. Chem. Soc., Chem. Commun.* (1988) 1322.
34. (a) Shaik, S. S. *New J. Chem. 7* (1983) 201; (b) Shaik, S. S. *J. Am. Chem. Soc. 105* (1983) 4359.
35. Ross, S. D., Finkelstein, M. and Petersen, R. C. *J. Am. Chem. Soc. 90* (1968) 6411.
36. Vitullo, V. P., Grabowski, J. and Sridharan, S. *J. Am. Chem. Soc. 102* (1980) 6463.
37. Halvorsen, A. and Songstad, J. *J. Chem. Soc., Chem. Commun.* (1978) 327.
38. Eaborn, C. and Jeffrey, J. C. *J. Chem. Soc.* (1954) 4266.
39. Cook, M. A., Eaborn, C. and Walton, D. R. M. *J. Organomet. Chem. 29* (1971) 389.
40. Ritchie, C. D. *J. Am. Chem. Soc. 105* (1983) 7313.
41. (a) Lund, T. and Lund, H. *Acta Chem. Scand., Ser. B 40* (1986) 470; (b) Lund, T. and Lund, H. *Acta Chem. Scand., Ser. B 42* (1988) 269; (c) Lund, H. and Kristensen, L. H. *Acta Chem. Scand., Ser. B 33* (1979) 495; (d) Lund, H. and Lund, T. *Tetrahedron Lett. 27* (1986) 95; (e) Daasbjerg, K., Lund, T. and Lund, H. *Tetrahedron Lett. 30* (1989) 493.
42. (a) Smith, G. F., Kuivila, H. G., Simon, R. and Sultan, L. *J. Am. Chem. Soc. 103* (1981) 833; (b) Kuivila, H. G. and Alnajjar, M. S. *J. Am. Chem. Soc. 104* (1982) 6146.
43. (a) Bordwell, F. G. and Harrelson, J. A., Jr. *J. Am. Chem. Soc. 109* (1987) 8112; (b) Bordwell, F. G. and Harrelson, J. A., Jr. *J. Am. Chem. Soc. 111* (1989) 1052; (c) Bordwell, F. G. and Wilson, C. A. *J. Am. Chem. Soc. 109* (1987) 5470.
44. Tanaka, J., Nojima, M. and Kusabayashi, S. *J. Am. Chem. Soc. 109* (1987) 3391.
45. Villar, H. O., Castro, E. A. and Rossi, R. A. *Z. Naturforsch., Teil A 39* (1984) 49.
46. Shaik, S. S. and Pross, A. *J. Am. Chem. Soc. 111* (1989) 4036.
47. (a) Julliard, M., Scagliarini, J. P., Rajzmann, M. and Chanon, M. *Chimia 40* (1986) 16; (b) Ashby, E. C. and Pham, T. N. *Tetrahedron Lett. 28* (1987) 3183.
48. Perrin, C. *J. Phys. Chem. 88* (1984) 3611.
49. Hayami, J.-I., Tanaka, N., Hihara, N. and Kaji, A. *Tetrahedron Lett.* (1973) 385.
50. Kaufmann, E., Schleyer, P. v. R., Houk, K. N. and Wu, Y.-D. *J. Am. Chem. Soc. 107* (1985) 5560.
51. Seebach, D. *Angew. Chem., Int. Ed. Engl. 27* (1988) 1624.
52. Herbert, E., Mazaleyart, J. P. and Welvart, Z. *New J. Chem. 9* (1985) 75.
53. Lexa, D., Savéant, J.-M., Su, K.-B. and Wang, D.-L. *J. Am. Chem. Soc. 110* (1988) 7617.
54. Clark, T. *Faraday Discuss. Chem. Soc. 78* (1984) 203.
55. Renaud, P. and Fox, M. A. *J. Am. Chem. Soc. 110* (1988) 5702.
56. Shalev, H. and Evans, D. H. *J. Am. Chem. Soc. 111* (1989) 2667.
57. Effenberger, F., Podszun, W., Schoeller, W. W. and Stohrer, W. D. *Chem. Ber. 109* (1976) 306.
58. Seebach, D., Imwinkelried, R. and Weber, T. *Mod. Synth. Methods 4* (1986) 125.
59. (a) Salem, L. and Rowland, C. *Angew. Chem., Int. Ed. Engl. 11* (1972) 92; (b) Shaik, S. S. *J. Am. Chem. Soc. 101* (1979) 3184.
60. Meyer, T. J. *Acc. Chem. Res. 22* (1989) 163.
61. Pross, A. and Chipman, D. *Free Radicals Biol. Med. 3* (1987) 55.

Received June 28, 1989.